Journal of Theoretical and Applied Vibration and Acoustics 7(1) 43-54(2021)

I S A V

Journal of Theoretical and Applied

Vibration and Acoustics

journal homepage: http://tava.isav.ir

Variations of ultrasonic wave attenuation in thick-walled cylinders subjected to a thermal gradient

R. Shabani [a], **F. Honarvar** [a,*]

[a]*NDE Lab, Faculty of Mechanical Engineering, K. N. Toosi University of Technology, 7 Pardis St., Mollasadra Ave., Vanak Sq., Tehran, Iran.*

ARTICLE INFO

Article history:
Received 14 February 2021

Received in revised form
5 April 2021

Accepted 23 June 2021

Available online 11 July 2021

Keywords:
Ultrasonic waves

Absolute attenuation

Thermal gradient

Thick-walled cylinder

Axial scanning

ABSTRACT

Accurate ultrasonic testing of engineering components like pressure vessels, which are subjected to extreme condition such as high stresses, high temperatures, and thermal gradients is important. Wave velocity and attenuation are two major parameters in ultrasonic testing. In this paper, a mathematical model is developed for calculation of the absolute attenuation of longitudinal waves in thick-walled cylinders that are subjected to thermal gradients. The cylinder is assumed to be homogeneous and isotropic. The independent variables are cylinder inner and outer radii, incidence angle and temperature of the inner surface of the cylinder in the range of 300-800 K. Based on the results obtained from the theoretical model, the wave attenuation is found to be highly sensitive to inner-surface temperature of the cylinder; however, the overall variation of the attenuation with respect to changes of the incidence angle and inner and outer radii of the cylinder is only 2 dB/m, which is ignorable in most practical applications. Furthermore, in the presence of a thermal gradient, there is an inverse relationship between the cylinder thickness and attenuation coefficient. The mathematical model is verified by using the experimental data available in the literature.

1. Introduction

Ultrasonic testing is a versatile nondestructive testing method for detecting defects and determining the properties of materials. Two major parameters in ultrasonic testing are wave velocity and attenuation. Attenuation is the loss of energy of the wave during its propagation in a material and has several applications including sizing and detection of microcracks [1-3]. Joshi

* Corresponding author:
E-mail address: honarvar@kntu.ac.ir (F. Honarvar)

http://dx.doi.org/10.22064/tava.2022.554349.1203

and Green Jr [4] observed that attenuation of ultrasonic waves is very sensitive to a fatigue damage in its early stages of development. Birring et al. [5] investigated changes in velocity and attenuation of ultrasonic waves in low-alloy steels due to hydrogen attack.

There are two types of attenuation, absolute attenuation and apparent attenuation. Apparent attenuation is comparative and relative; in other words, the shape of the specimen, the probe, and

the coupling are remained unchanged while the amplitude of the back-wall echoes are compered [6]. Absolute attenuation is indicative of the intrinsic nature of the material and to measure it, specimen geometry, sound beam divergence, instrumentation, and procedural effects should be taken into account. These results can be achieved with more specialized ultrasonic equipment and techniques [7]. Absolute attenuation of ultrasonic waves depends on the chemical composition and microstructure of the material in which the wave propagates [8]. The material microstructure is a function of temperature; therefore, the absolute attenuation of ultrasonic waves is also a function of temperature. There are several studies on the effect of temperature on the attenuation of ultrasonic waves. Papadakis [9] investigated the effect of austenitizing temperature on the velocity and attenuation of ultrasonic waves in SAE 52100 steel. He found that the main reason for weakening of the waves in this type of steel is grain scattering. Bamber and Hill [10] investigated the effect of temperature on the velocity and attenuation of ultrasonic waves within the frequency range of 1-7 MHz in soft tissues of human body in a temperature range of 5-65 °C. Rajendran et al. [11] developed a low-cost setup for measuring the velocities and attenuation coefficients of ultrasonic waves in solids in a temperature range of 300-580 K. Thuy et al. [12] investigated the velocity and attenuation of longitudinal and transverse ultrasonic waves in X40H, S45, SCM420 and SCR420 steels in a temperature range of 0-50 °C.

Thick-walled cylinders are widely utilized in different industries including petroleum and chemical industries. They usually work under extreme conditions such as high temperatures and high pressures. If hot fluids run through a pipe or chemical reactions take place within a cylinder, [13, 14], the inner surface of the cylinder becomes much hotter than its outer surface temperature and a thermal gradient is created across the cylinder wall. To accurately test these cylinders by ultrasonic method, the effect of thermal gradient on the attenuation coefficient should be taken into account. In the existence of a thermal gradient, the temperature is not the same at different points. Moreover, the absolute attenuation coefficient varies with temperature variations; therefore, when there is a thermal gradient, the attenuation coefficient differs at different locations. Ultrasonic testing of pipes can be carried out in either axial or circumferential directions [15].

In this paper, a mathematical model is developed for estimating the absolute attenuation of ultrasonic longitudinal waves in a thick-walled cylinder which is under a thermal gradient during axial scanning. The effects of incidence angle, inner surface temperature and inner and outer radii of the cylinder on wave attenuation are also studied by using the developed model.

2. Theory

In this Section, we try to develop a mathematical model for variations of the absolute attenuation of ultrasonic waves. The two variables R_i and R_o are the inner and outer radii of the cylinder, respectively. The inside and outside temperatures are designated as T_i and T_o, respectively, where $T_i > T_o$. The temperature distribution is governed by the following equation [16]:

$$T(R) = p \ln R + q \tag{1}$$

where radius R lies somewhere between R_i and R_o. The boundary conditions for calculation of constant coefficients p and q are:

$$T(R_o) = T_o \tag{2}$$

$$T(R_i) = T_i \tag{3}$$

By using Eqs. (1) and (2), we have:

$$T(R) = p \ln\left(\frac{R}{R_o}\right) + T_o \tag{4}$$

Equation (4) is the radial temperature distribution across the wall thickness of the cylinder. By using Eqs. (3) and (4), the coefficient p is found to be:

$$p = \frac{T_i - T_o}{\ln\left(\frac{R_i}{R_o}\right)} \tag{5}$$

The cylinder axial cross-sectional view and incidence angle γ are shown in Fig. 1. A longitudinal wave is transmitted into the cylinder and passes through a differential element dR which is located at radius R.

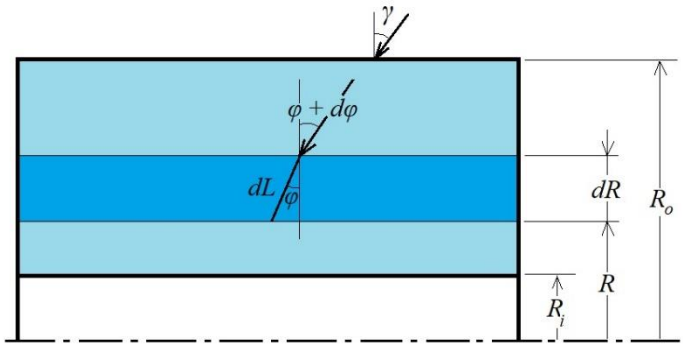

Fig. 1. The cylinder axial cross-sectional view

Due to the small thickness of the differential element, its temperature is considered to be constant and equal to T. The incidence angle and the refraction angle of the differential element are chosen as $\varphi + d\varphi$ and φ, respectively [17]. As shown in Fig. 1, dL is the wave travel path inside the differential element. According to the geometry shown in Fig. 1, we can write:

$$dL = -\frac{dR}{\cos\varphi} \tag{6}$$

A negative sign appears in the right-hand-side of Eq. (6) because the two differential increments dR and dL are in opposite directions, i.e., radius increases upwards while travel path increases downwards. The wave attenuation coefficient inside the element is called α. The attenuation coefficient is a function of wave frequency f, and temperature T [8, 18]:

$$\alpha = \alpha(T, f) \tag{7}$$

From Eqs. (4) and (7), we have:

$$\alpha = \alpha(R, f) \tag{8}$$

which gives the wave attenuation coefficient as a function of radius and frequency. The amplitudes of the waves at Ri and Ro are assumed to be Ai and Ao, respectively. As the ultrasonic wave travels through the wall of the cylinder, its amplitude decreases continuously; therefore, since the wave travels from the outer surface towards the inner surface of the cylinder, we get:

$$A(R) = A \tag{9}$$

$$A(R + dR) = A + dA \tag{10}$$

In Eq. (9), A is the amplitudes of the waves at radius R. The wave attenuation coefficient, α, inside the element can be calculated from Eq. 11 [18]:

$$\frac{A + dA}{A} = e^{\alpha(-dL)} \tag{11}$$

Since dA and dL have opposite directions (amplitude increases upwards while travel path increases downwards), a negative sign appears in the power of the exponential term in the right-hand-side of Eq. (11). The right-hand-side of Eq. (11) can be written as a power series [19]:

$$e^{-\alpha dL} = \sum_{n=0}^{\infty} \frac{(-\alpha dL)^n}{n!} = 1 - \alpha dL + \frac{1}{2}(\alpha dL)^2 - \frac{1}{3}(\alpha dL)^3 + \cdots \tag{12}$$

Since dL is infinitesimal, higher order terms tend to zero much more rapidly. By dropping the higher order terms and keeping the first two terms in Eq. (12), we have:

$$e^{-\alpha dL} \approx 1 - \alpha dL \tag{13}$$

By placing Eqs. (6) and (13) in Eq. (11), we obtain:

$$\frac{dA}{A} = -\alpha dL = \frac{\alpha dR}{\cos\varphi} \tag{14}$$

Now, by integrating Eq. (14) we have:

$$\int_{A_o}^{A_i} \frac{dA}{A} = \int_{R_o}^{R_i} \frac{\alpha dR}{\cos\varphi} \tag{15}$$

which can be written as:

$$\ln\frac{A_i}{A_o} = \int_{R_o}^{R_i} \frac{\alpha dR}{\cos\varphi} \tag{16}$$

Using Snell's law, the angle φ is determined from the following equation [17]:

$$\varphi = \sin^{-1}\left(\frac{c_e}{c_s}\sin\gamma\right) \tag{17}$$

where, c_s is the surrounding medium wave velocity and c_e is the differential element wave velocity. The velocity c_e can be calculated from [17]:

$$c_e = c_o \sqrt{(1 + \frac{\beta p}{E_o} \ln \frac{R}{R_o})(1 + 3\sigma p \ln \frac{R}{R_o})} \tag{18}$$

where, E_o and c_o designate Young's modulus and ultrasonic wave velocity at temperature T_o, respectively. The constant σ is the thermal expansion coefficient and β accounts for temperature effects on Young's modulus.

Let's call the total path traveled by the wave along the cylinder axis $L_{\gamma\text{-}axial}$. The wave average attenuation coefficient in the axial direction is also called $\alpha_{\gamma\text{-}axial}$. The distance $L_{\gamma\text{-}axial}$ can be calculated from [17]:

$$L_{\gamma-axial} = \int_{R_o}^{R_i} -\frac{dR}{\cos \varphi} \tag{19}$$

the average absolute attenuation coefficient $\alpha_{\gamma\text{-}axial}$ can be obtained from [18]:

$$\alpha_{\gamma-axial} = -\frac{1}{L_{\gamma-axial}} \ln \frac{A_i}{A_o} \tag{20}$$

Combining Eqs. (16), (19) and (20), the average attenuation coefficient $\alpha_{\gamma\text{-}axial}$ can be written as:

$$\alpha_{\gamma-axial} = \frac{\int_{R_o}^{R_i} \frac{\alpha dR}{\cos \varphi}}{\int_{R_o}^{R_i} \frac{dR}{\cos \varphi}} \tag{21}$$

Equation (21) gives the average attenuation coefficient when there the cylinder experiences a thermal gradient.

3. Results and discussion

A cylinder which is made from structural steel is considered. The values of E_o and c_o are measured according to ASTM E494-15.

Table 1. The values of E_o and c_o for structural steel at 295 K

Parameter	E_o (Pa)	$c_{o\text{-Longitudinal}}$ (m/s)
Value	210.8×10^9	5926.5

Table 2. Values of constant β [20]

T (K)	β (Pa/K)
295-400	-52.76×10^6
295-500	-62.36×10^6
295-600	-74.84×10^6
295-700	-94.3×10^6
295-800	-125.88×10^6

Table 3. Thermal expansion coefficient at different temperature ranges [21]

T (K)	σ (1/K)
273-373	12.2×10^{-6}
273-673	13.4×10^{-6}
273-873	14.2×10^{-6}

Absolute (material) attenuation at 20 MHz for a longitudinal ultrasonic wave traveling in structural steel at various temperatures is given in Table 4.

Table 4. Absolute attenuation of structural steel at different temperatures [8]

T (K)	α (dB/m)
290	4
378	8
441	12
506	18
645	28
728	30
796	37
878	37
923	38
961	44
992	52

Using Chauvenet's criterion [22], we found that one of the data points in [8] was an outlier and therefore, it was removed from Table 4. By fitting a line to the data given in Table 4, we get:

$$\alpha(T) = 0.0616T - 14.2 \quad \text{(at 20 MHz)} \qquad 290 \leq T \leq 992 \tag{22}$$

The correlation coefficient, r, for this linear fit is 0.985 and $r^2 = 0.9706$, which indicates that the line fit for this data is reliable [22]. Water is assumed to be the medium surrounding the cylinder.

3.1. Radii Ro and Ri

To study the influence of variations of outer radius on $\alpha_{\gamma\text{-axial}}$, we set T_o = 300 K, T_i = 800 K, R_i = 0.1 m and $\gamma = 5°$. Figure 2 shows the variations in $\alpha_{\gamma\text{-axial}}$ as a function of outer radius R_o.

Figure 2 shows that by increasing R_o in the range of 0.11-0.2 m, the attenuation of the longitudinal wave decreases slightly. The overall decrease is approximately 1.5 dB/m in axial scanning. If R_i is fixed as R_o increases, the difference between the distance traveled by the wave in regions with temperatures exceeding the average temperature becomes less than the distance traveled in regions with temperatures below the average temperature. [17]. On the other hand, from Eq. (22), the attenuation decreases as temperature decreases. Consequently, the attenuation coefficient $\alpha_{\gamma\text{-axial}}$ decreases as R_o increases. To examine the effect of variations of R_i on $\alpha_{\gamma\text{-axial}}$, we set T_o = 300 K, T_i = 800 K, R_o = 0.2 m and $\gamma = 5°$. Figure 3 shows the variations in $\alpha_{\gamma\text{-axial}}$ as a function of inner radius R_i.

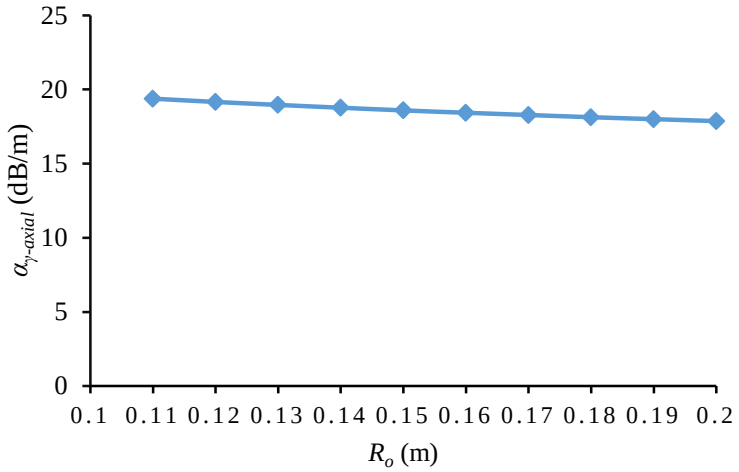

Fig. 2. Variations in $\alpha_{\gamma\text{-}axial}$ versus outer radius R_o

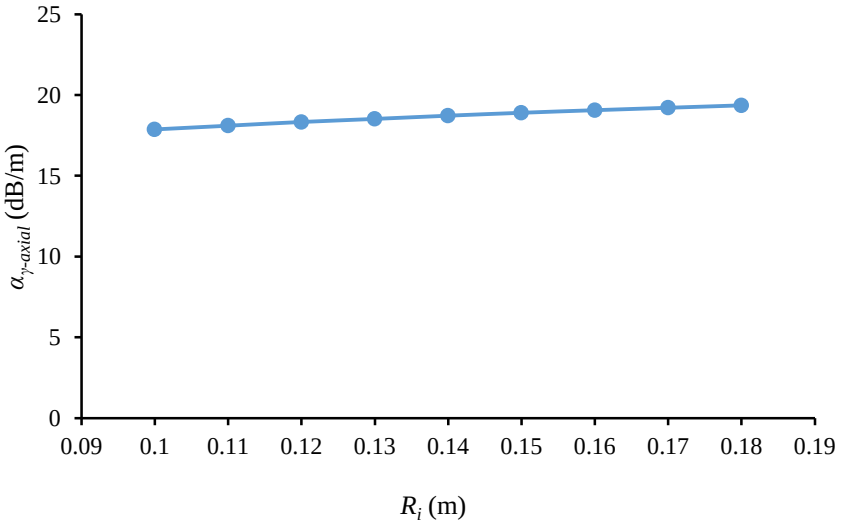

Fig. 3. Variations in $\alpha_{\gamma\text{-}axial}$ versus inner radius R_i

Figure 3 shows that by increasing the inner radius R_i from 0.1 to 0.18 m, the attenuation of the longitudinal waves increases slightly, and the overall increase is approximately 1.5 dB/m. If R_o is fixed as R_i increases, most of the wave path falls within the regions whose temperature is more than the average temperature. [17]. On the other hand, from Eq. (22), the attenuation decreases with the decline of temperature and consequently, the attenuation coefficient $\alpha_{\gamma\text{-}axial}$ increases as R_i is increased. From Figs. 2 and 3, there is an inverse relationship between cylinder thickness (ΔR) and attenuation coefficient $\alpha_{\gamma\text{-}axial}$; in other words, as the thickness of the cylinder increases in the presence of a thermal gradient, the attenuation coefficient decreases.

3.2. Incidence angle γ

To study the influence of the incidence angle on attenuation coefficient $\alpha_{\gamma\text{-axial}}$, we set T_o and T_i equal to 300 K and 800 K and R_i and R_o equal to 0.1 m and 0.2 m, respectively. Figure 4 shows the variations of $\alpha_{\gamma\text{-axial}}$ with respect to the incidence angle γ.

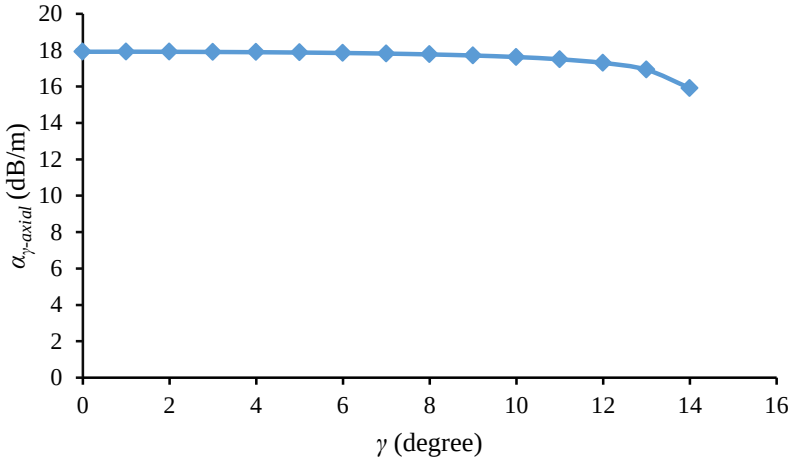

Fig. 4. Variations of $\alpha_{\gamma\text{-axial}}$ versus wave incidence angle

The first critical angle for structural steel is 14.47°. Two regions can be observed in Fig. 4. In the first region, as incidence angle is increased (but still much less than the critical angle), the attenuation slightly decreases. In the second region, where incidence angle is approaching the critical angle, the wave attenuation declines more rapidly. As γ increases the travel path also increases and the difference between the distance traveled by the wave in regions with temperatures less than the average-temperature becomes longer than the distance traveled in regions with temperatures more than the average-temperature. Therefore, the attenuation coefficient $\alpha_{\gamma\text{-axial}}$ decreases as γ increases. Furthermore, the overall decrease is approximately 2 dB/m in axial scanning.

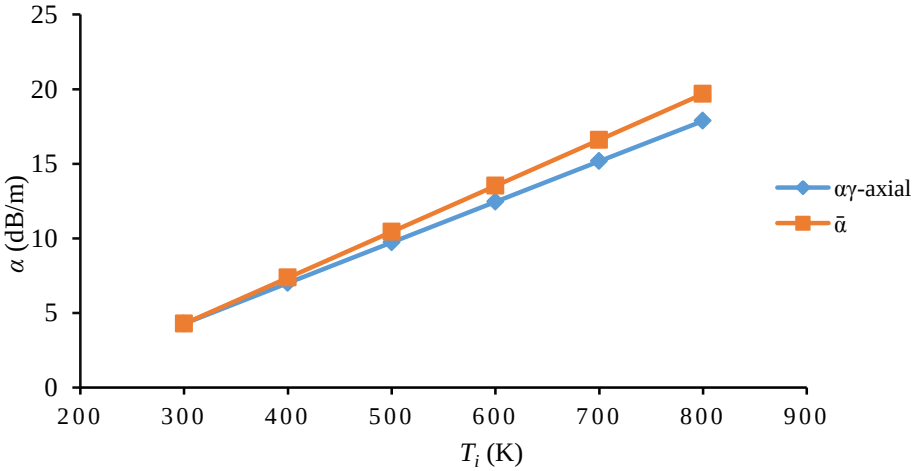

Fig. 5. Variations in $\alpha_{\gamma\text{-axial}}$ and $\bar{\alpha}$ versus temperature T_i

3.3. Temperature T_i

The influence of temperature T_i on $\alpha_{\gamma\text{-}axial}$ is investigated when the temperature T_o is set to 300 K. The inner and outer radii and the incidence angle are taken as 0.1 m, 0.2 m, and 5°, respectively. In Fig. 5, $\alpha_{\gamma\text{-}axial}$ and $\bar{\alpha}$ (= ($\alpha(T_i)$+$\alpha(T_o)$)/2) is plotted versus T_i.

The values of σ and β are available for a range of 300-800 K; therefore, this temperature range is considered in Fig. 5. In Fig. 5, both $\alpha_{\gamma\text{-}axial}$ and $\bar{\alpha}$ increase with increase of T_i. When the temperature T_o is kept constant, by increasing T_i, the average temperature of the cylinder also increases. Equation (22) shows that the temperature and attenuation vary proportionally, i.e., as temperature increases, attenuation also increases. As a result, as T_i increases, the average temperature also increases and leads to an increase in attenuation. According to Fig. 5, the difference between $\alpha_{\gamma\text{-}axial}$ and $\bar{\alpha}$ also increases with increase of T_i, however in the temperature range considered, the maximum difference is only 1.8 dB/m (at T_i =800 K) which is not significant in practical applications and can be ignored (especially at lower temperatures):

$$\alpha_{\gamma-axial} \cong \bar{\alpha} \tag{23}$$

Table 5. Comparison of the measured values of $\bar{\alpha}_{\text{Experiment}}$ and calculated values of $\alpha_{\gamma-axial}$ for R_i = 0.19 m

No.	T_o (K)	T_i (K)	$\bar{T}$ (K)	$\alpha_{\gamma-axial} \cong \bar{\alpha}_{\text{Theory}}$ (dB/m)	$\bar{\alpha}_{\text{Experiment}}$ (dB/m)	$Error$ dB/m	%
1	295	461	378	9	8	1	13
2	295	587	441	12.8	12	0.8	7
3	400	612	506	16.9	18	1.1	6
4	500	790	645	25.4	28	2.6	9
5	666	790	728	30.6	30	0.6	2
6	792	800	796	34.8	37	2.2	6

4. Verification of the model

To verify the validity of the developed model, we consider Eq. (23) and the case of a normally incident wave (γ = 0). Since no experimental results are available for thick-walled cylinders in the literature, we use the experimental data reported in [8] for a plate made from structural steel. It should be noted that absolute attenuation is independent of work-piece geometry (at uniform and constant temperature) and depends on the intrinsic nature of the material [7]. Absolute attenuation coefficient, $\bar{\alpha}$, is measured on a 20-mm thick steel plate at several different temperatures in [8]. The theoretical values of $\alpha_{\gamma-axial}$ and $\bar{\alpha}_{\text{Theory}}$ are calculated from Eqs. (21) and (23) which were developed in Sections 2 and 3. Since [8] provides the values of $\bar{\alpha}$ at several distinct temperatures, the values of $\bar{\alpha}_{\text{Expriment}}$ are presented at six different temperatures in Tables 5 to 7. In Tables 5-7, the temperatures T_i and T_o are chosen such that their mean value equals the mean temperature $\bar{T}$ reported in [8]. In Tables 5 to 7, the values of R_i and R_o are

chosen such that their difference (ΔR) is equal to the thickness of the plate, i.e., 0.02 m. A cylinder is thick-walled if its thickness is greater than 1/10 of its internal radius [23]. Therefore, considering the plate thickness of 0.02 m used in experiments, Ri should be equal to 0.2 m or less for the cylinder to be considered as thick-walled. We examine three different values of R_i which are 0.19, 0.1, and 0.02 (all less than 0.2 m) and find the values of $\alpha_{\gamma-axial}$ and compare them with experimental values of $\bar{\alpha}_{\text{Expriment}}$.

Table 6. Comparison of the measured values of $\bar{\alpha}_{\text{Experiment}}$ and calculated values of $\alpha_{\gamma-axial}$ for R_i = 0.1 m

No.	T_o (K)	T_i (K)	$\bar{T}$ (K)	$\alpha_{\gamma-axial} \cong \bar{\alpha}_{\text{Theory}}$ (dB/m)	$\bar{\alpha}_{\text{Experiment}}$ (dB/m)	$Error$ dB/m	%
1	295	461	378	8.9	8	0.9	11
2	295	587	441	12.7	12	0.7	6
3	400	612	506	16.8	18	1.2	7
4	500	790	645	25.3	28	2.7	10
5	666	790	728	30.5	30	0.5	2
6	792	800	796	34.8	37	2.2	6

Table 7. Comparison of the measured values of $\bar{\alpha}_{\text{Experiment}}$ and calculated values of $\alpha_{\gamma-axial}$ for R_i = 0.02 m

No.	T_o (K)	T_i (K)	$\bar{T}$ (K)	$\alpha_{\gamma-axial} \cong \bar{\alpha}_{\text{Theory}}$ (dB/m)	$\bar{\alpha}_{\text{Experiment}}$ (dB/m)	$Error$ dB/m	%
1	295	461	378	8.5	8	0.5	6
2	295	587	441	11.9	12	0.1	1
3	400	612	506	16.2	18	1.8	10
4	500	790	645	24.5	28	3.5	13
5	666	790	728	30.2	30	0.2	1
6	792	800	796	34.8	37	2.2	6

Tables 5 to 7 show that the model is in good agreement with experimental results for all considered temperature gradients. The maximum error is %13, but in most cases, errors are less than 10%. This error can be attributed mostly to the uncertainties in measurements.

5. Conclusion

In this paper, a mathematical model was developed for estimating the absolute attenuation of ultrasonic waves in thick-walled cylinders when the cylinder is experiencing a thermal gradient. The inner and outer radii, the incidence angle and the inner-surface temperature of the cylinder

were considered as independent variables and how they affect the ultrasonic wave attenuation $\alpha_{\gamma\text{-}axial}$ was studied. The outcome of the theoretical model was in good agreement with experimental results reported in the literature. From the theoretical results of the model, it can be stated that the wave attenuation is extremely sensitive to inner-surface temperature of the cylinder. Therefore, in practical applications, if considerable variations in observed in inner-surface temperature, the the thermal gradient should be taken into account in conducting the measurements. Furthermore, in the presence of a thermal gradient, there is an inverse relationship between cylinder thickness (ΔR) and attenuation coefficient $\alpha_{\gamma\text{-}axial}$. The overall variation of the attenuation with respect to the changes of the incidence angle and inner and outer radii of the cylinder is approximately 2 dB/m, which can be ignored in most practical applications.

6. Conflict of interest

On behalf of all authors, the corresponding author states that there is no conflict of interest.

References

[1] H. Willems, K. Goebbels, Characterization of microstructure by backscattered ultrasonic waves, Metal Science, 15 (1981) 549-553.
[2] D.K. Mak, Determination of grain size, hysteresis constant and scattering factor of polycrystalline material using ultrasonic attenuation, Canadian Metallurgical Quarterly, 25 (1986) 253-255.
[3] A.B. Bouda, S. Lebaili, A. Benchaala, Grain size influence on ultrasonic velocities and attenuation, Ndt & E International, 36 (2003) 1-5.
[4] N.R. Joshi, R.E. Green Jr, Ultrasonic detection of fatigue damage, Engineering Fracture Mechanics, 4 (1972) 577-583.
[5] A. Birring, M. Bartlett, K. Kawano, Ultrasonic detection of hydrogen attack in steels, Corrosion, 45 (1989) 259-263.
[6] J. Krautkrämer, H. Krautkrämer, Ultrasonic testing by determination of material properties, in: Ultrasonic Testing of Materials, Springer, 1990, pp. 528-550.
[7] R. Store, Practice for the Measurement of the apparent Attenuation of longitudinal Ultrasonic Waves by Immersion Method, ASTM Section, 3 (1991) 263-265.
[8] C. Scruby, B. Moss, Non-contact ultrasonic measurements on steel at elevated temperatures, NDT & E International, 26 (1993) 177-188.
[9] E.P. Papadakis, Ultrasonic attenuation and velocity in SAE 52100 steel quenched from various temperatures, Metallurgical Transactions, 1 (1970) 1053-1057.
[10] J.C. Bamber, C. Hill, Ultrasonic attenuation and propagation speed in mammalian tissues as a function of temperature, Ultrasound in medicine & biology, 5 (1979) 149-157.
[11] V. Rajendran, N. Palanivelu, B. Chaudhuri, A device for the measurement of ultrasonic velocity and attenuation in solid materials under different thermal conditions, Measurement, 38 (2005) 248-256.
[12] T.M.T. Luong, V.T. Pham, X.T. Nguyen, D.A. Nguyen, T.H.T. Nguyen, Temperature Dependence of Ultrasonic Waves Properties Propagated in Some Types of Carbon Steels, VNU Journal of Science: Mathematics-Physics, 33 (2017).
[13] A. Kosugi, Y. Ono, I. Matsuya, I. Ihara, Application of laser ultrasound to noncontact temperature profiling of a heated hollow cylinder, in: Journal of Physics: Conference Series, IOP Publishing, 2014, pp. 012015.
[14] S. Kamal, U.S. Dixit, A. Roy, Q. Liu, V.V. Silberschmidt, Comparison of plane-stress, generalized-plane-strain and 3D FEM elastic–plastic analyses of thick-walled cylinders subjected to radial thermal gradient, International Journal of Mechanical Sciences, 131 (2017) 744-752.
[15] G. ASTM, 52-00. Standard Practice for Exposing and Evaluating Metals and Alloys in Surface Seawater, West Conshohocken, PA: ASTM International, (2020).
[16] A. Bejan, A.D. Kraus, Heat transfer handbook, John Wiley & Sons, 2003.

[17] R. Shabani, F. Honarvar, Development of a mathematical model for propagation of ultrasonic waves in thick-walled cylinders in the presence of a thermal gradient–Case of axial scanning, Ultrasonics, 119 (2022) 106628.
[18] D.E. Bray, R.K. Stanley, Nondestructive evaluation: A tool in design, manufacturing, and service, CRC press, 2018.
[19] R.A. Silverman, Modern calculus and analytic geometry, Courier Corporation, 2002.
[20] G. Li, P. Wang, Advanced analysis and design for fire safety of steel structures, Springer Science & Business Media, 2013.
[21] M. Handbook, Properties and selection: Irons steels and high performance alloys, Vol. 1; ASM International, Handbook Committee, (1990).
[22] R.S. Figliola, D.E. Beasley, Theory and design for mechanical measurements, John Wiley & Sons, 2020.
[23] B. Phalguna, Stress and failure analysis of thick walled cylinder with oblique hole, Int J Eng Res Technol, 6 (2017) 36-45.